Title: Effects of glyphosate and aminomethylphosphonic acid on an isogeneic model of the human blood-brain barrier

Authors: Adriana Martinez, Abraham Jacob Al-Ahmad

PII: S0378-4274(18)31904-0
DOI: https://doi.org/10.1016/j.toxlet.2018.12.013
Reference: TOXLET 10389

To appear in: *Toxicology Letters*

Received date: 17 September 2018
Revised date: 10 December 2018
Accepted date: 28 December 2018

Please cite this article as: Martinez A, Al-Ahmad AJ, Effects of glyphosate and aminomethylphosphonic acid on an isogeneic model of the human blood-brain barrier, *Toxicology Letters* (2018), https://doi.org/10.1016/j.toxlet.2018.12.013

Effects of glyphosate and aminomethylphosphonic acid on an isogeneic model of the human blood-brain barrier

Adriana Martinez, Abraham Jacob Al-Ahmad*

Department of Pharmaceutical Sciences, Texas Tech University Health Sciences Center, School of Pharmacy, Amarillo, TX, United States of America

* Corresponding author:

Abraham Al-Ahmad, PhD

Department of Pharmaceutical Sciences

Texas Tech University Health Sciences Center, School of Pharmacy

1300 South Coulter Street, Amarillo TX 79119, United States of America

Tel: +1 806 414 9369

email: abraham.al-ahmad@ttuhsc.edu

Highlights

- Glyphosate and AMPA can affect the blood-brain barrier integrity.
- Glyphosate can diffuse across the blood-brain barrier.
- Low glyphosate levels (<1µM) has no detrimental acute or chronic effect on iPSC-derived neurons.
- High doses of GPH and AMPA (100µM) can affect BMECs glucose uptake and neurons metabolic activity.

Abstract

Glyphosate is a pesticide used for occupational and non-occupational purposes. Because glyphosate targets a metabolic pathway absent in animals, it is considered safe for humans. Yet, case reports of accidental exposure to concentrated solutions following self-inflicted poisoning documented neurological lesions suggesting a neurotoxicity. In this study, we investigated the effect of acute exposure to glyphosate (GPH) on the blood-brain barrier *in vitro* based on induced pluripotent stem cells (iPSCs) and compared to two chemical analogs: aminomethylphosphonic acid (AMPA) and glycine (GLY), for concentrations ranging from 0.1µM to 1000µM. GPH treatment (1 and 10µM) for 24 hours showed an increase BBB permeability to fluorescein, with similar outcomes for AMPA. In addition to its ability to disrupt the barrier function, GPH show evidence of permeability across the BBB. Although no detrimental effects were observed on neuron differentiation at high doses, we noted changes in neuronal cell metabolic activity and glucose uptake in brain microvascular endothelial cells (BMECs) following treatment with 100µM GPH or AMPA. Taken together, our data indicates that accidental exposure to high level of GPH may result in neurological damage via an opening of the blood-brain barrier and an alteration of glucose metabolism.

Keywords

Glyphosate; blood-brain barrier; neurons; induced pluripotent stem cells.

Introduction

Glyphosate (N-phosophonomethylglycine, GPH) (Henderson et al., 2010; Scholl-Burgi et al., 2008) is a glycine derivative used as an occupational and non-occupational herbicide. GPH mechanism of action occurs via targeting of the shikimic acid pathway, a biosynthetic pathway absents from animals. Specifically, its biological activity occurs via the inhibition of the 5-enolpyruvylshikimate-3-phosphate (EPSP) synthase. Coupled with its very low oral toxicity in rats (LD_{50} oral>4320 mg/kg) (Birch, 1993), GPH is considered as a safe herbicide. Although GPH present in commercial and concentrated solutions is commonly present as a mixture containing surfactants as a saline form (e.g. glyphosate isoproprylamine salt), the ability of such surfactants to cross the GI tract concomitantly with GPH remains undocumented. However, it is estimated that only 35-40% of GPH given per oral route is absorbed (Brewster et al., 1991). Upon absorption, glyphosate fate in humans is considered mostly occurring as its non-metabolized fraction, with only a small fraction (<0.6%) is being metabolized into aminomethylphosphonic acid (AMPA) as reported by Hori and colleagues (Hori et al., 2003). GPH apparent half-life is estimated to be 3.1 hours (Roberts et al., 2010) and considered to be eliminated mostly via renal route (Brewster et al., 1991). Despite its relative safety, there are several case reports in the literature of self-inflicted poisoning by ingestion of commercial formulation of glyphosate (e.g. Roundup®) (Hori et al., 2003; Kamijo et al., 2016; Picetti et al., 2018; Potrebic et al., 2009; Roberts et al., 2010; Talbot et al., 1991; Yu et al., 2017; Zouaoui et al., 2013). Aside from gastrointestinal effects associated with the ingestion of such preparations, several studies highlighted neurological effects associated with GPH poisoning including altered consciousness (Lee et al., 2017; Zouaoui et al., 2013) or presence of neurological lesions (Nishiyori et

al., 2014). In addition to neurological effects observed in patients, several studies highlighted the presence of a neurotoxicity associated with GPH *in vitro* (Alloisio et al., 2015; Coullery et al., 2016; Culbreth et al., 2012) and *in vivo* (Roy et al., 2016). However, the presence of similar neurotoxicity due to AMPA, the main metabolite of GPH remains undocumented. Interestingly, a study by Lee and colleagues (Lee et al., 2017) reported an increase of S100β serum levels in patients within 24 hours after ingestion, such elevation maybe indicative of a possible opening of the blood-brain barrier (BBB) (Foerch et al., 2007; Kanner et al., 2003; Kapural et al., 2002). Yet, the effect of GPH at the BBB remains undocumented. In this study, we investigated the effect of GPH on the barrier function using an isogeneic model based on patient-derived induced pluripotent stem cells (iPSCs) (Lippmann et al., 2014; Lippmann et al., 2012; Patel et al., 2017). In this study, we investigated the biological activity of GPH and compared it to AMPA, its metabolite and to glycine, an amino acid sharing structural similarity with GPH.

Materials and Methods

Cell culture:

IMR90-c4 iPSC (RRID: CVCL_C437) line was purchased from WiCell cell repository (WiCell, Madison, WI) (Yu et al., 2007). Undifferentiated iPSC colonies were maintained on hPSC-grade growth factor reduced Matrigel (C-Matrigel, Corning, Corning, MA) in presence of Essential 8 medium (E8, ThermoFisher, Waltham, MA).

iPSC differentiation into BMECs and neurons:

iPSCs were differentiated into BMECs following the protocol established by Lippmann and colleagues (Lippmann et al., 2014; Lippmann et al., 2012) iPSCs were seeded as single cells on T-Matrigel (Trevigen, Gaithersburg, MD) at a cell density of 20'000 cells/cm^2 in E8 supplemented with 10μM Y-27632 (Tocris, Minneapolis, MN). 24 hours after seeding, cells were maintained in E8 for 5 days prior to differentiation. Cells were maintained for 6 days in unconditioned medium (UM: DMEM/F12 with 15mM HEPES (ThermoFisher), 20% knockout serum replacement (KOSR, Thermofisher), 1% non-essential amino acids (Thermofisher), 0.5% Glutamax (Thermofisher) and 0.1mM β-mercaptoethanol (Sigma-Aldrich). After 6 days, cells were incubated for 2 days in presence of EC$^{+/+}$ (EC medium (Thermofisher) supplemented with 1% platelet-poor derived serum (PDS, Alfa-Aesar, Thermofisher), 20ng/mL human recombinant basic fibroblast growth factor (bFGF, Tocris, Abingdon, United Kingdom) and 10μM retinoic acid (Sigma-Aldrich)). After such maturation process, cells were dissociated by Accutase® (Corning) treatment and seeded as single cells on tissue-culture plastic surface (TCPS) coated with a solution of collagen from human placenta (Sigma-Aldrich) and bovine plasma fibronectin (Sigma-Aldrich) (80μg/cm^2 and 20μg/cm^2 respectively). Twenty-four hours after seeding, cells were incubated in presence of EC$^{-/-}$ (EC medium supplemented with 1% PDS). Barrier phenotype experiments were performed 48 hours after seeding. The differentiation of iPSCs into neurons using an adherent three-step differentiation method. Undifferentiated iPSCs were allowed to grow on C-Matrigel for 4 days prior to differentiation. Differentiation of these iPSCs into neural stem cells (NSCs) was induced using neural induction medium (NIM, Thermofisher) for 11 days (Yan et al., 2013). After such induction period, NSCs were enzymatically dissociated by Accutase

and seeded as single cells at a cell density of 100'000 cells/cm^2 in presence of 10μM Y-27632 on C-Matrigel coated plates. Twenty-four hours after seeding, NSCs were further differentiated into neural precursor cells (NPCs) by incubating them in presence of neural differentiation medium (NDM: human pluripotent stem cell serum-free medium (Thermofisher), supplemented with 2% bovine serum albumin (BSA, Thermofisher), 1% Glutamax I (Thermofisher), 10μg/mL human recombinant brain-derived neurotrophic growth factor (BDNF, Thermofisher) and 10μg/mL human recombinant glial-derived neurotrophic factor (GDNF, Thermofisher)) for 5 days (Efthymiou et al., 2014). Differentiation of these NPCs into neurons was achieved by seeding 50'000 cells/cm^2 on TCPS-coated plates. Neurons were seeded on poly-D-lysine (2μg/cm^2, Sigma)/laminin (1μg/cm^2, Sigma) coated plates and maintained in neuron maturation medium (NMM: Neurobasal-A medium, 2% B27 supplement, 1% CultureOne supplement (Thermofisher) and 1% fetal bovine serum (Thermofisher)). In both cases, medium was replaced every 2 days for 14 to 16 days. Co-culture experiments were performed by seeding iPSC-derived BMECs at day 8 of differentiation on inserts juxtaposed over 16-days iPSC-derived neurons. BMECs were maintained in EC medium, whereas neurons were maintained in NMM medium.

Glyphosate, AMPA and glycine treatment:

Glyphosate (GPH, EPA 547 1000μg/mL solution), aminomethylphosphonic acid (AMPA) and glycine (GLY) were obtained as analytical grade reagents (Sigma-Aldrich, St. Louis, MO) and stored as recommended. Dilutions were performed immediately before experiments and maintained in cell medium for 24 hours or 48 hours. In co-culture

experiments, compounds were added in the apical chamber at a concentration of 100μM and incubated for 6 hours. iPSC-derived neurons monocultures exposed to similar concentrations served as controls.

Cell metabolic activity:

Following treatment, CellTiter Aqueous® MTS reagent ([3-(4,5-dimethylthiazol-2-yl)-5-(3-carboxymethoxyphenyl)-2-(4-sulfophenyl)-2H-tetrazolium, inner salt Promega, Madison, WI) was added in each sample following recommendation by the manufacturer. Cells were maintained for 60 minutes at 37ºC following by a measurement of the absorbance at 490nm using an ELISA plate reader (SynergyMX2, BioTek Instruments, Winooski, VT). Absorbance obtained from samples were subtracted from background absorbance and normalized against controls (untreated cells).

iPSC-derived BMECs barrier function:

iPSC-derived BMECs were seeded on Transwells (polyester, 0.4μm pore size, Corning) and coated as previously described. iPSC-derived BMECs were seeded at a seeding density of 10^6 cells/cm^2. Barrier function was assessed 48 hours after seeding for iPSC-derived BMECs monolayers. Barrier tightness was measured by assessing both the transendothelial electrical resistance (TEER) and paracellular diffusion. TEER was measured using an EVOHM STX2 chopstick electrode (World Precision Instruments, Sarasota, FL). For each experiment, three measurements were performed for each

insert and the average resistance obtained was used for the determination of the barrier function.

Fluorescein, glyphosate and mannitol permeability assay:

To assess changes in paracellular permeability, sodium fluorescein (Sigma-Aldrich) was added in the apical (top) chamber at a final concentration of 10µM. 100µL aliquots were sampled from the basolateral (donor) chamber every 15 minutes for up to 60 minutes. Each aliquot sample were replaced with 100µL of cell medium. Fluorescein content in samples was assessed using a fluorimeter ELISA plate reader (SynergyMX2). Glyphosate permeability assay was assessed by incubating cells in presence of 100µM GPH dissolved in $EC^{-/-}$ in the apical chamber. Sampling in the basolateral chamber occurred as previously mentioned. GPH detection was performed by derivation and spectrophotometric detection using a validated method (Waiman et al., 2012). Borax solution (40mmol/L) was prepared from a stock solution (40g/L, LabChem, Zelienople, PA), whereas FMOC-Cl solution (1g/L) was prepared by dissolving FMOC-Cl in acetonitrile (Fisher Reagents, Thermofisher). Samples were alkalinized by addition of 17µl of Borax followed by the addition of 17µl of FMOC-Cl solution. Samples were allowed to incubate in the dark under gentle shaking for 2 hours. The derivation process was terminated by adding 137µL dichloromethane (Fisher Reagents), homogenized and centrifuged at 2000 rpms for 5 minutes. The organic phase was recovered and analyzed by spectrophotometer at 265nm using a quartz cuvette (length: 1 cm). Blank $EC^{-/-}$ medium was used as blank, whereas GPH dissolved in $EC^{-/-}$ at concentrations ranging from 10nM to 10µM were used to establish a GPH standard curve.

In experiments involving mannitol permeability, [^{14}C] D-mannitol (Perkin Elmer) (1g/L, total activity of 1Ci/mL) was added in the apical chamber. Sampling in the basolateral chamber occurred as previously mentioned. β-emission was assessed by adding 5mL ScintiSafe 30% liquid scintillation cocktail (Fisher Chemicals, Thermofisher) and counted using a Beckman-Coulter LS6500 liquid scintillation counter (Beckman-Coulter, Pasadena, CA). For all three molecules, permeability across BMECs monolayers were obtained by calculating the clearance slope from both samples and blank inserts and by calculation of the Pe value following the method of Perriere and colleagues (Perriere et al., 2005).

Immunocytochemistry:

Cells were stained on TCPS plates and fixed with 4% paraformaldehyde (Electron Microscopy Sciences, Hatfield, PA). Cells were blocked for 1 hour at room temperature in PBS-G (PBS supplemented with 10% normal goat serum (Sigma-Aldrich)) with 0.2% Triton-X100. Cells were incubated overnight in presence of claudin-5 (RRID:AB_2533200), occludin (RRID:AB_2533101), GLUT1 (RRID:AB_10979643) or βIII tubulin (RRID:AB_262133). Cells were washed with PBS containing 1% bovine serum album (BSA, Sigma-Aldrich), and incubated in presence of Alexa Fluor®-488 conjugated secondary antibodies (1:200, Thermofisher) for 1 hour at room temperature. Cells were counterstained with DAPI (Sigma-Aldrich) and observed on a Leica inverted epifluorescence microscope (Leica). Micrograph pictures were acquired using Leica Acquisition Suite X (Leica) and processed using ImageJ. Semi-quantitative analysis was measured by measuring the average fluorescence intensity of each micrograph pictures

using the built-in measure tool in ImageJ (ImageJ software, NIH, Bethesda, MD). Average fluorescence values from negative controls were subtracted from fluorescence values obtained in samples.

Flow cytometry:

iPSC-derived BMECs at Day 10 of differentiation were treated with 100µM GPH, AMPA or GLY for 24 hours. Cells were harvested by enzymatic dissociation using Accutase® (Corning) and fixed with 4% paraformaldehyde. Cells were blocked in PBS-G supplemented with 0.2% Triton-X dissolved in PBS for 30 minutes, following by an overnight incubation at 4ºC in primary antibody solution (GLUT-1, SPM498, 1:100; dissolved in PBS-G. Cells were washed with PBS containing 1% BSA and incubated in presence of Alexa Fluor® 555-conjugated antibody (1:200, Life Technology). As isotype control, we exposed cells in presence of mouse IgG as primary antibody. Cells were analyzed using a BD FACSVerse® (Becton-Dickinson, Franklin Lakes, NJ, USA), with fluorescence PMT adjusted to IgG isotype control, fluorescence intensity for each sample was obtained from a count of 10’000 cellular events. Median fluorescence intensity (MFI, geometric mean) was determined for each sample and corrected against IgG isotype.

Glucose and doxorubicin uptake assay:

Glucose uptake assays were performed by incubating cells grown on TCPS in presence of cell medium supplemented with [^{14}C] D-glucose (Perkin Elmer; total activity=1µCi/mL). Cells were incubated for 60 minutes at 37ºC. Following such incubation period, cells were briefly washed three times with ice-cold PBS and

homogenized with PBS+0.2% Triton-X 100 (Sigma-Aldrich) for 10 minutes. Samples radioactivity was assessed by adding 100µL samples with 5mL ScintiSafe 30% liquid scintillation cocktail (Fisher Chemicals, Thermofisher) and counted using a Beckman-Coulter LS6500 liquid scintillation counter (Beckman-Coulter, Pasadena, CA). Doxorubicin uptake assay was performed by pre-incubating iPSC-derived BMECs in presence of GPH, AMPA or GLY at 100µM concentrations for 2 hours. Doxorubicin (Sigma-Aldrich) was added a 5µM final concentration and allowed to incubate for 1 hour. Cells were homogenized as previously described and total fluorescence assessed by fluorimetry (SynergyMX2). Total protein content obtained from cell homogenates were determined using a BCA protein assay (Pierce, Thermofisher).

Statistics:

Cells were randomly assigned treatment conditions prior each experiment. Data are represented as mean ± S.D. from three or more independent experiments. One-way analysis of the variance (ANOVA) coupled with Dunnett (or Kruskal-Wallis) tests analysis were performed using Prism 7.0 built-in package (GraphPad Software, La Jolla, CA). A $P<0.05$ p-value was considered as indicative of a statistic difference between one or more groups.

Results

Effects of glyphosate and AMPA on BMECs cell viability

We firstly assessed the impact of glyphosate (GPH) on BMECs cell monolayers viability using a range of concentrations partially overlapping levels found in patients reported as

asymptomatic (17µM), minor and moderate (241µM and 428µM respectively) by Roberts and colleagues (Roberts et al., 2010). Treatment with GPH for 24 hours at concentrations ranging from 10µM to 1000µM resulted in no changes in cell metabolic activity (Fig.1A). Similar outcomes were observed using AMPA or glycine (GLY). Taken together, our data indicates that glyphosate or AMPA unlikely have toxicity towards the blood-brain barrier.

Glyphosate and AMPA affect fluorescein permeability in BMECs monolayers

Next, we investigated changes in the barrier function in such BMECs monolayers using TEER and fluorescein permeability (Fig.1B&C). In addition to the previous concentrations, we included two concentrations (0.1 and 1µM) ranges aimed to reflect average plasma concentrations reported in occupational exposure (Pan et al., 2016). No changes in TEER were noted for any of the concentrations tested. Neither AMPA or GLY showed effects on TEER. However, we noticed a biphasic response in our model. At 0.1µM, we noted a slight decrease in fluorescein permeability for all three groups (GPH, AMPA and GLY), followed by a significant increase for both GPH and AMPA at 1 and 10µM. Notably, higher concentrations resulted in permeability values similar to controls. To confirm the increase in paracellular profile observed with GPH, we investigated changes in paracellular permeability using [^{14}C]-mannitol, an alternative paracellular flux marker (Fig.1D). We observed a modest but significant increase in mannitol permeability following treatment with 10µM GPH. In contrast, no significant increase was noted following AMPA or GLY treatment. In summary, our data suggest

that GPH and AMPA treatment may increase the barrier permeability in BMECs monolayers.

High levels of glyphosate, AMPA and glycine impair tight junction complexes integrity

To better understand the effect of GPH and AMPA on the barrier function, we investigated changes in in tight junction complexes, in particular changes in claudin-5 and occludin, by immunocytochemistry (Figure 2). We did not observe changes in claudin-5 immunolocalization following GPH or AMPA treatment (Fig.2A), however we noted a dose-dependent decrease in claudin-5 relative expression (as quantified by fluorescence intensity) in all groups (Fig.2B). Treatment with GPH resulted in decreased claudin-5 fluorescence intensity at 100 and 1000µM concentrations, whereas treatment with AMPA marked a significant decrease already by 10µM concentration. GLY treatment showed a significant decrease at 100 and 1000µM concentrations.

To confirm such observation, we investigated changes in occludin levels (Fig.2C&D). As expected, no changes in occludin localization occurred following treatment (Fig.2C). However, we noted a significant decrease in occludin protein levels (as marked by reduced fluorescence intensity) in all groups with the exception of the 10µM GLY treatment group. Unlike claudin-5, such effect appeared dose-independent as we have noted no changes between 10µM treatment and higher concentrations. Taken together, our data suggest that GPH may increase paracellular permeability in BMECs monolayers to fluorescein via partial disruption of tight junction complexes integrity.

Glyphosate diffuses across the blood-brain barrier via a transcellular route, modulates glucose uptake in BMECs

In addition to its effect on paracellular permeability, we investigated the ability of GPH to cross the BBB. Thus we investigated the diffusion profile of GPH following an acute exposure at 100µM in the apical chamber and measured its diffusion for 2 hours (Fig.3A&B) and quantified the amount of GPH present in the basolateral chamber using the analytical method developed by Waiman and colleagues (Waiman et al., 2012). At 2 hours of diffusion, the amount of GPH capable to cross BMECs monolayers was about 1.67±0.31% of the injected dose (100µM). In addition, the permeability value of GPH was significantly higher than fluorescein (18.67±3.55 x 10^{-6}cm/min versus 10.59 x 10^{-6}cm/min) or mannitol (13.10±2.03 x 10^{-6} cm/min) in cells treated with the same amount of GPH (Fig.3B). In conclusion, our data suggests that GPH may cross the BBB via a transcellular mechanism. Next, we investigated the effect of GPH and AMPA on drug efflux transporters using doxorubicin as a drug efflux substrate (Fig.3C). With the exception of AMPA that showed a two-fold increase over control, treatment with 100µM GPH or GLY for 24 hours showed no differences compared to controls. Finally, we investigated changes in GLUT1 localization and expression (the main glucose transporter at the blood-brain barrier) in BMECs following treatment by immunocytochemistry (Fig.3D), as previous studies reported changes in glucose levels in certain vertebrates following exposure to GPH and AMPA. (Becker et al., 2009; Kondera et al., 2018). We noted changes in GLUT1 immunoreactivity following treatment with GPH, with an apparent increase following treatment with 100µM. Similar behavior was observed with AMPA albeit subtler. Notably, we noted a notable increase

in GLUT1 immunoreactivity following treatment with 100 and 1000µM GLY. Such observation was confirmed by assessing GLUT1 fluorescence intensity in our monolayers (Fig.3E). To ensure such differences was not inherent to the technique, we performed a flow cytometry analysis (Fig.3F&G) and compared changes in mean fluorescence indexes following treatment with 100µM for 24 hours. Notably, GPH treatment yielded an increase in GLUT1 expression levels compared to control (Fig.3G). Although AMPA showed no differences in GLUT1 expression, treatment with GLY resulted in a significant decrease compared to control. Finally, we measured changes in glucose uptake in BMECs monolayers, using [^{14}C]-D-glucose (Fig.3H). We noted a progressive increase in glucose uptake with a maximum uptake at 100µM concentration. AMPA showed a similar pattern than GPH, resulting in a 3-fold increase compared to control in the 100µM. GLY treatment resulted in the highest increase in glucose uptake as noted at 100 and 1000 µM concentrations. Taken together, our data suggest that exposure to high levels of GLY or AMPA may impair glucose uptake and metabolism in BMECs monolayers via an alteration in GLUT1 expression and/or activity.

Neurons co-cultured with brain microvascular endothelial cells display an impaired cell metabolic activity

As GPH showed ability to cross the BBB and yielded to changes in GLUT1 expression and glucose uptake in BMECs monolayers, we investigated the effects of GPH on neurovascular coupling using a BMEC/neurons co-culture model (Fig.4) based on our previous publication (Patel et al., 2017). We firstly, assessed the ability of such co-

cultures to yield to tighter barrier function by measuring differences in TEER between BMECs monocultures and BMECs co-cultured with iPSC-derived neurons (Fig.4A). As expected, co-cultures significantly up-regulated the barrier tightness, as we noted a 3-fold increase in TEER in BMECs co-cultured with neurons compared to BMECs maintained in monocultures. Next, these co-cultures to 100μM GPH, AMPA or GLY by adding these compounds on the apical (top) chamber for 24 hours. Addition of these compounds on the apical chamber did not significantly alter the barrier tightness as we noted no differences in TEER (Fig.4B). As expected, we noted a mild increase in fluorescein permeability (Fig.4C) in GPH-treated group compared to control, but not in the AMPA or GLY groups. Finally, we investigated the effect GPH incubation in the apical chamber (100μM) on the neurovascular coupling, by investigating changes in neuronal cell metabolic activity by MTS (Fig.4D) following 6 hours exposure. Notably, we noticed a significant decrease in cell metabolic activity in neurons co-cultured compared to monocultures. Following incubation with GPH in the apical chamber, we noticed an increase in cell metabolic activity compared to control. By contrast, neurons directly exposed to monocultures showed no sign of activity. Interestingly, we observed a similar increase in cell metabolic activity compared control. Such changes observed in GPH was also observed in AMPA co-cultures but not in GLY co-cultures. Following such incubation, we investigated changes in gross morphology of iPSC-derived neurons colonies by immunocytochemistry against βIII-tubulin (Tuj1, Fig.4E). We did not observe macroscopic changes in iPSC-derived neurons following incubation with GPH, AMPA or GLY both in monocultures and co-cultures, suggesting that changes in cell metabolic

activity is unlikely due to cell death. In conclusion, our data suggest that exposure to high amount of GPH (100µM) may impair neurovascular coupling.

GPH and AMPA effect on neuron progenitor cells

As we have demonstrated the ability of GPH to cross the BBB and to alter the neurovascular unit, we investigated the effect of GPH on differentiating and differentiated neurons (Fig.5) by exposing cells to a concentration considered representative of the amount crossing the BBB (0.1-1µM). We firstly investigated the effect of acute exposure (24 hours) on the cellular metabolic activity of undifferentiated NPCs by MTS assay (Fig.5A). Although we did not observe any differences in cell metabolic activity at 0.1µM, we noted a significant decrease in MTS activity at 1µM in both GPH and GLY groups, suggesting a possible deleterious effect on NPC cell viability. Nevertheless, immunofluorescence analysis of these NPCs (Fig.5B) showed no major alterations in the relative cell density and nestin (a cellular marker of neural stem cells/progenitor cells) immunoreactivity. To further confirm the innocuity of GPH and AMPA on neurogenesis, we treated differentiating NPCs continuously for 16 days (by replacing cell medium every 48 hours) in presence of 0.1µM GPH, AMPA or GLY. Such concentration was chosen to be representative of plasma concentration reported in occupational workers and 20 times higher than values reported in non-occupational population (Conrad et al., 2017; Pan et al., 2016). Chronic exposure (16 days) to low GPH levels (0.1µM) We did not observe significant changes in the cell metabolic activity between the different groups compared to controls (Fig.5C). In addition to changes in cell metabolic activity, we investigated changes in gross morphology in iPSC-derived

neurons colonies (Fig.5D). After 16 days, we observed the presence of a dense neurite network. Treatment with GPH or AMPA did not display major changes in gross morphology of iPSC-derived neuron colonies, as we still observed presence of dense neurite network. In conclusion, chronic exposure to low-levels of GPH or AMPA failed to show any signs of neurotoxicity.

Glyphosate and AMPA affects neurons cell metabolism without showing detrimental effects on neurites density.

Finally, we investigated the effect of acute exposure by treating iPSC-derived neurons seeded at low density (50'000 cells/cm^2) in presence of GPH or AMPA for 24 hours at concentrations ranging from 1μM to 1000μM (Fig.4E-H). Treatment with GPH and AMPA showed a decrease in cell metabolic activity upon exposure to GPH to 10μM and higher concentrations (Fig.5E). AMPA showed similar outcomes than GPH, albeit not statistically significant. Treatment with GLY showed little effects on cell metabolic activity. To better such changes in cell metabolic activity with cellular distress, we investigated changes in cell density and neurites formation by immunocytochemistry (Fig.5F). With the exception of GLY group, no depletion in neurites was observed in both GPH and AMPA groups. Upon quantification of cell nuclei and neurites per surface area (Fig.5G&H), we noted a progressive decrease in neuron density for both GPH and AMPA (Fig.5G), with a significant decrease noted at 1000μM. However, no differences in terms of neurites density were noted in GPH and AMPA groups, with the exception of very high amount of GLY (100 and 1000μM treatment). Taken together, our data

suggest that low concentrations (<10μM) of GPH and AMPA may not have detrimental effects on iPSC-derived neurons.

Discussion

In this study, we investigated the toxicity of acute glyphosate poisoning on the blood-brain barrier integrity by investigating its activity on the different cell types of the neurovascular unit. To reflect the situation of a self-inflicted poisoning exposure, we treated cells with glyphosate and AMPA concentration ranges from 10μM to 1000μM. Such concentration ranges are within GPH plasma values reported by Roberts and colleagues from patients with self-inflicted poisoning exposure and scored from asymptomatic (17μM) to fatal (8.12mM) at the time of admission in clinic (Roberts et al., 2010). We consider it important that the meaning of such concentration such values are put into context. According to the literature, the average GPH and AMPA levels measured in urine following non-occupational exposure (residual pesticide exposure) in North America were 0.28μg/L and 0.30μg/L (1.6nM and 2.7nM respectively) respectively (McGuire et al., 2016); while a study by Conrad and colleagues (Conrad et al., 2017) showed an average GPH and AMPA amount of GPH and AMPA of 0.78μg/L and 0.64μg/L (4.6nM and 5.7nM respectively) in urine samples from a non-occupational German cohort. By contrast, occupational workers showed higher values of GPH and AMPA, with average plasma levels of 11.73μg/L and 5.29μg/L (69nM and 117nM) for GPH and AMPA respectively (Pan et al., 2016). As a reference, normal plasma GLY concentrations range from 125 to 450μM, with values below 20μM for CSF (Applegarth et al., 1979; Van Hove et al., 1993). We noted an increase in fluorescein permeability

for both GPH and AMPA at 1μM and 10μM. We noted similar outcome for mannitol in cells exposed to 1μM GPH. Such observation is suggesting a possible detrimental effect of GPH and AMPA on the barrier function. Although we did not observe major changes in tight junction complexes localization, we noted a decrease in both claudin-5 and occludin protein levels by immunoreactivity for all three groups. Such observations suggest that GPH and AMPA may interfere with tight junction complexes integrity. Yet, the interference of such compounds on tight junction proteins remains unclear. We speculate that a possible mechanism explaining such down-regulation maybe occurring via shedding of such proteins by matrix metalloproteinases (MMPs). MMPs are proteases well documented to cleave claudin-5 and occludin during neurological diseases (e.g. ischemic stroke)(Feng et al., 2011; Liu et al., 2012; Yang et al., 2007). Thus, we will further investigate the effect of GPH and AMPA on tight junction proteins expression and MMPs activity in BMECs.

An interesting observation done in our study was an increase in permeability following GLY treatment. Although we did not observe a statistical significance, we sill noted a 50% increase in paracellular permeability following GLY treatment at 100 and 1000μM. Interestingly, a study recently reported the case report of an increased BBB permeability in a patient suffering from glycine encephalopathy (also known as nonketotic hyperglycinemia (NKH)) and presenting a meningitis (Scholl-Burgi et al., 2008). Our data suggest that high levels of GLY may increase the permeability of the BBB and disrupt tight junction complexes in such range. Therefore, assessing the barrier function in BMECs derived from iPSCs obtained from these patients would provide important insights on the effect of hyperglycinemia on the blood-brain barrier integrity. In addition

to changes in barrier function, we assessed GPH permeability in our BMECs monolayers. We estimate that about 1% of the injected dose (100μM) diffused across BMECs monolayers (data not shown). However, the permeability for GPH was significantly higher than fluorescein despite its high hydrophilicity (xLogP=-4.63). Although its permeability value was higher than mannitol, we did not observe a statistical difference. Thus, we speculate that GPH cross the BBB via a carrier-mediated diffusion. A recent study suggested the possible involvement of system L-type amino acid transporters 1 and 2 (LAT1/LAT2 encoded by *SLC7A5* and *SLC7A8* genes respectively) in the uptake of GPH in mammalian cells (Xu et al., 2016), two receptors expressed at the BBB (Kido et al., 2001). A major limitation of our study is the limited access to LC-MS chromatography, limiting our scope to provide a further understanding of the diffusion of GPH and AMPA. Therefore, a long-term goal will focus on detailing the permeability of GPH and AMPA and the contribution of LAT1 and LAT2 in such diffusion. Amongst the different cell types, neurons displayed the most important changes in metabolic activity following exposure to GPH and AMPA. We noticed significant changes in neuronal cell metabolic activity following treatment with GPH, AMPA or GLY whereas we did not observe significant changes in BMECs. Yet, such decrease in cell metabolic was unlikely reflective of a neurotoxicity, as we noted no changes in neuronal cell density and neurites formation. Assessing the effects of GPH and AMPA on iPSC-derived glycinergic neurons coupled with electrophysiological methods would provide important insights on the ability of GPH and AMPA to act as glycine mimetic molecules. A change in cell metabolic activity observed in our cells may be due to changes in glucose metabolism, as we noted changes in glucose uptake in

BMECs, as well as some changes in GLUT1 expression levels. Glyphosate has been associated with changes in glucose serum levels in various fish species (Becker et al., 2009; Kondera et al., 2018), yet there are no reports in the presence of such effects in mammalian species. Therefore, further studies investigating the effect of glyphosate and AMPA on brain glucose uptake and changes in glucose and lactate CSF levels *in vivo* is needed to confirm our observation. Taken together, our data demonstrate the relative safety of glyphosate and AMPA on the blood-brain barrier during acute accidental exposure. Yet, the presence of an active uptake and diffusion of glyphosate across the blood-brain barrier suggests the need of an extensive brain-centered pharmacokinetic studies to evaluate the pharmacokinetics and pharmacodynamics of glyphosate on the central nervous system during acute exposure and in individuals exposed to high amount of such pesticides. In conclusion, our study further supports the relative safety of GPH with minimal effects observed at concentrations significantly higher than baseline exposure levels, occupational and non-occupational alike.

Acknowledgements

This study was funded by Texas Tech University Health Sciences Center institutional funds to A.A. The authors have no conflict of interests to disclose.

References

Alloisio, S., Nobile, M., Novellino, A., 2015. Multiparametric characterisation of neuronal network activity for in vitro agrochemical neurotoxicity assessment. Neurotoxicology 48, 152-165.
Applegarth, D.A., Edelstein, A.D., Wong, L.T., Morrison, B.J., 1979. Observed range of assay values for plasma and cerebrospinal fluid amino acid levels in infants and children aged 3 months to 10 years. Clin Biochem 12, 173-178.
Becker, A.G., Moraes, B.S., Menezes, C.C., Loro, V.L., Santos, D.R., Reichert, J.M., Baldisserotto, B., 2009. Pesticide contamination of water alters the metabolism of juvenile silver catfish, Rhamdia quelen. Ecotoxicol Environ Saf 72, 1734-1739.
Birch, M., 1993. Toxicological investigation of CP 67573-3. In: Office of Prevention, P., and Toxic Substances, (Ed.). U.S. Government Printing Office, Washington, DC.
Brewster, D.W., Warren, J., Hopkins, W.E., 2nd, 1991. Metabolism of glyphosate in Sprague-Dawley rats: tissue distribution, identification, and quantitation of glyphosate-derived materials following a single oral dose. Fundam Appl Toxicol 17, 43-51.
Conrad, A., Schroter-Kermani, C., Hoppe, H.W., Ruther, M., Pieper, S., Kolossa-Gehring, M., 2017. Glyphosate in German adults - Time trend (2001 to 2015) of human exposure to a widely used herbicide. Int J Hyg Environ Health 220, 8-16.
Coullery, R.P., Ferrari, M.E., Rosso, S.B., 2016. Neuronal development and axon growth are altered by glyphosate through a WNT non-canonical signaling pathway. Neurotoxicology 52, 150-161.
Culbreth, M.E., Harrill, J.A., Freudenrich, T.M., Mundy, W.R., Shafer, T.J., 2012. Comparison of chemical-induced changes in proliferation and apoptosis in human and mouse neuroprogenitor cells. Neurotoxicology 33, 1499-1510.
Efthymiou, A., Shaltouki, A., Steiner, J.P., Jha, B., Heman-Ackah, S.M., Swistowski, A., Zeng, X., Rao, M.S., Malik, N., 2014. Functional screening assays with neurons generated from pluripotent stem cell-derived neural stem cells. Journal of biomolecular screening 19, 32-43.
Feng, S., Cen, J., Huang, Y., Shen, H., Yao, L., Wang, Y., Chen, Z., 2011. Matrix metalloproteinase-2 and -9 secreted by leukemic cells increase the permeability of blood-brain barrier by disrupting tight junction proteins. PLoS One 6, e20599.
Foerch, C., Wunderlich, M.T., Dvorak, F., Humpich, M., Kahles, T., Goertler, M., Alvarez-Sabin, J., Wallesch, C.W., Molina, C.A., Steinmetz, H., Sitzer, M., Montaner, J., 2007. Elevated serum S100B levels indicate a higher risk of hemorrhagic transformation after thrombolytic therapy in acute stroke. Stroke 38, 2491-2495.
Henderson, A.M., Gervais, J.A., Luukinen, B., Buhl, K., Stone, D., 2010. Glyphosate Technical Fact Sheet. National Pesticide Information Center. Oregon State University Extension Services.
Hori, Y., Fujisawa, M., Shimada, K., Hirose, Y., 2003. Determination of the herbicide glyphosate and its metabolite in biological specimens by gas chromatography-mass spectrometry. A case of poisoning by roundup herbicide. J Anal Toxicol 27, 162-166.
Kamijo, Y., Takai, M., Sakamoto, T., 2016. A multicenter retrospective survey of poisoning after ingestion of herbicides containing glyphosate potassium salt or other glyphosate salts in Japan. Clin Toxicol (Phila) 54, 147-151.

Kanner, A.A., Marchi, N., Fazio, V., Mayberg, M.R., Koltz, M.T., Siomin, V., Stevens, G.H., Masaryk, T., Aumayr, B., Vogelbaum, M.A., Barnett, G.H., Janigro, D., 2003. Serum S100beta: a noninvasive marker of blood-brain barrier function and brain lesions. Cancer 97, 2806-2813.
Kapural, M., Krizanac-Bengez, L., Barnett, G., Perl, J., Masaryk, T., Apollo, D., Rasmussen, P., Mayberg, M.R., Janigro, D., 2002. Serum S-100beta as a possible marker of blood-brain barrier disruption. Brain Res 940, 102-104.
Kido, Y., Tamai, I., Uchino, H., Suzuki, F., Sai, Y., Tsuji, A., 2001. Molecular and functional identification of large neutral amino acid transporters LAT1 and LAT2 and their pharmacological relevance at the blood-brain barrier. J Pharm Pharmacol 53, 497-503.
Kondera, E., Teodorczuk, B., Lugowska, K., Witeska, M., 2018. Effect of glyphosate-based herbicide on hematological and hemopoietic parameters in common carp (Cyprinus carpio L). Fish Physiol Biochem.
Lee, J.W., Choi, Y.J., Park, S., Gil, H.W., Song, H.Y., Hong, S.Y., 2017. Serum S100 protein could predict altered consciousness in glyphosate or glufosinate poisoning patients. Clin Toxicol (Phila) 55, 357-359.
Lippmann, E.S., Al-Ahmad, A., Azarin, S.M., Palecek, S.P., Shusta, E.V., 2014. A retinoic acid-enhanced, multicellular human blood-brain barrier model derived from stem cell sources. Scientific reports 4, 4160.
Lippmann, E.S., Azarin, S.M., Kay, J.E., Nessler, R.A., Wilson, H.K., Al-Ahmad, A., Palecek, S.P., Shusta, E.V., 2012. Derivation of blood-brain barrier endothelial cells from human pluripotent stem cells. Nat Biotechnol 30, 783-791.
Liu, J., Jin, X., Liu, K.J., Liu, W., 2012. Matrix metalloproteinase-2-mediated occludin degradation and caveolin-1-mediated claudin-5 redistribution contribute to blood-brain barrier damage in early ischemic stroke stage. J Neurosci 32, 3044-3057.
McGuire, M.K., McGuire, M.A., Price, W.J., Shafii, B., Carrothers, J.M., Lackey, K.A., Goldstein, D.A., Jensen, P.K., Vicini, J.L., 2016. Glyphosate and aminomethylphosphonic acid are not detectable in human milk. Am J Clin Nutr 103, 1285-1290.
Nishiyori, Y., Nishida, M., Shioda, K., Suda, S., Kato, S., 2014. Unilateral hippocampal infarction associated with an attempted suicide: a case report. J Med Case Rep 8, 219.
Pan, L., Xu, M., Yang, D., Wang, B., Zhao, Q., Ding, E.-M., Zhu, B., 2016. The association between coronary artery disease and glyphosate exposure found in pesticide factory workers. Public Health and Emergency 1, 9-9.
Patel, R., Page, S., Al-Ahmad, A.J., 2017. Isogenic blood-brain barrier models based on patient-derived stem cells display inter-individual differences in cell maturation and functionality. J Neurochem 142, 74-88.
Perriere, N., Demeuse, P., Garcia, E., Regina, A., Debray, M., Andreux, J.P., Couvreur, P., Scherrmann, J.M., Temsamani, J., Couraud, P.O., Deli, M.A., Roux, F., 2005. Puromycin-based purification of rat brain capillary endothelial cell cultures. Effect on the expression of blood-brain barrier-specific properties. J Neurochem 93, 279-289.
Picetti, E., Generali, M., Mensi, F., Neri, G., Damia, R., Lippi, G., Cervellin, G., 2018. Glyphosate ingestion causing multiple organ failure: a near-fatal case report. Acta Biomed 88, 533-537.

Potrebic, O., Jovic-Stosic, J., Vucinic, S., Tadic, J., Radulac, M., 2009. [Acute glyphosate-surfactant poisoning with neurological sequels and fatal outcome]. Vojnosanit Pregl 66, 758-762.
Roberts, D.M., Buckley, N.A., Mohamed, F., Eddleston, M., Goldstein, D.A., Mehrsheikh, A., Bleeke, M.S., Dawson, A.H., 2010. A prospective observational study of the clinical toxicology of glyphosate-containing herbicides in adults with acute self-poisoning. Clin Toxicol (Phila) 48, 129-136.
Roy, N.M., Carneiro, B., Ochs, J., 2016. Glyphosate induces neurotoxicity in zebrafish. Environ Toxicol Pharmacol 42, 45-54.
Scholl-Burgi, S., Korman, S.H., Applegarth, D.A., Karall, D., Lillquist, Y., Heinz-Erian, P., Davidson, A.G., Haberlandt, E., Sass, J.O., 2008. The relation of cerebrospinal fluid and plasma glycine levels in propionic acidaemia, a 'ketotic hyperglycinaemia'. Journal of inherited metabolic disease 31, 395-398.
Talbot, A.R., Shiaw, M.H., Huang, J.S., Yang, S.F., Goo, T.S., Wang, S.H., Chen, C.L., Sanford, T.R., 1991. Acute poisoning with a glyphosate-surfactant herbicide ('Roundup'): a review of 93 cases. Hum Exp Toxicol 10, 1-8.
Van Hove, J., Coughlin, C., II, Scharer, G., 1993. Glycine Encephalopathy. In: Adam, M.P., Ardinger, H.H., Pagon, R.A., Wallace, S.E., Bean, L.J.H., Stephens, K., Amemiya, A. (Eds.) GeneReviews((R)), Seattle (WA).
Waiman, C.V., Avena, M.J., Garrido, M., Band, B.F., Zanini, G.P., 2012. A simple and rapid spectrophotometric method to quantify the herbicide glyphosate in aqueous media. Application to adsorption isotherms on soils and goethite. Geoderma 170, 154-158.
Xu, J., Li, G., Wang, Z., Si, L., He, S., Cai, J., Huang, J., Donovan, M.D., 2016. The role of L-type amino acid transporters in the uptake of glyphosate across mammalian epithelial tissues. Chemosphere 145, 487-494.
Yan, Y., Shin, S., Jha, B.S., Liu, Q., Sheng, J., Li, F., Zhan, M., Davis, J., Bharti, K., Zeng, X., Rao, M., Malik, N., Vemuri, M.C., 2013. Efficient and rapid derivation of primitive neural stem cells and generation of brain subtype neurons from human pluripotent stem cells. Stem Cells Transl Med 2, 862-870.
Yang, Y., Estrada, E.Y., Thompson, J.F., Liu, W., Rosenberg, G.A., 2007. Matrix metalloproteinase-mediated disruption of tight junction proteins in cerebral vessels is reversed by synthetic matrix metalloproteinase inhibitor in focal ischemia in rat. J Cereb Blood Flow Metab 27, 697-709.
Yu, G.C., Jian, X.D., Gao, B.J., 2017. [The clinical analytics of 10 patients with acute glyphosate poisoning]. Zhonghua Lao Dong Wei Sheng Zhi Ye Bing Za Zhi 35, 382-383.
Yu, J., Vodyanik, M.A., Smuga-Otto, K., Antosiewicz-Bourget, J., Frane, J.L., Tian, S., Nie, J., Jonsdottir, G.A., Ruotti, V., Stewart, R., Slukvin, II, Thomson, J.A., 2007. Induced pluripotent stem cell lines derived from human somatic cells. Science 318, 1917-1920.
Zouaoui, K., Dulaurent, S., Gaulier, J.M., Moesch, C., Lachatre, G., 2013. Determination of glyphosate and AMPA in blood and urine from humans: about 13 cases of acute intoxication. Forensic Sci Int 226, e20-25.

Figure Legends

Figure 1: Effects of glyphosate and AMPA on the blood-brain barrier integrity

Effect of prolonged exposure to glyphosate (GPH), AMPA and glycine (GLY) on the barrier integrity in IMR90-derived BMECs monolayers. Cells were exposed for various concentrations for 24 hours, followed by measurement of changes in cell metabolic activity by MTS (A) and in the barrier function by TEER (B) and permeability to sodium fluorescein (C) and mannitol (D). Note the quasi-absence of effect on cell metabolism (A), whereas we noted an increased fluorescein permeability at 1μM and 10μM for both GPH and AMPA, whereas we noted an increase in mannitol permeability in 10μM GPH treatment only. Scale bar = 50μm. N=3 per group, * and ** denotes $P<0.05$ and $P<0.01$ versus control respectively.

Figure 1

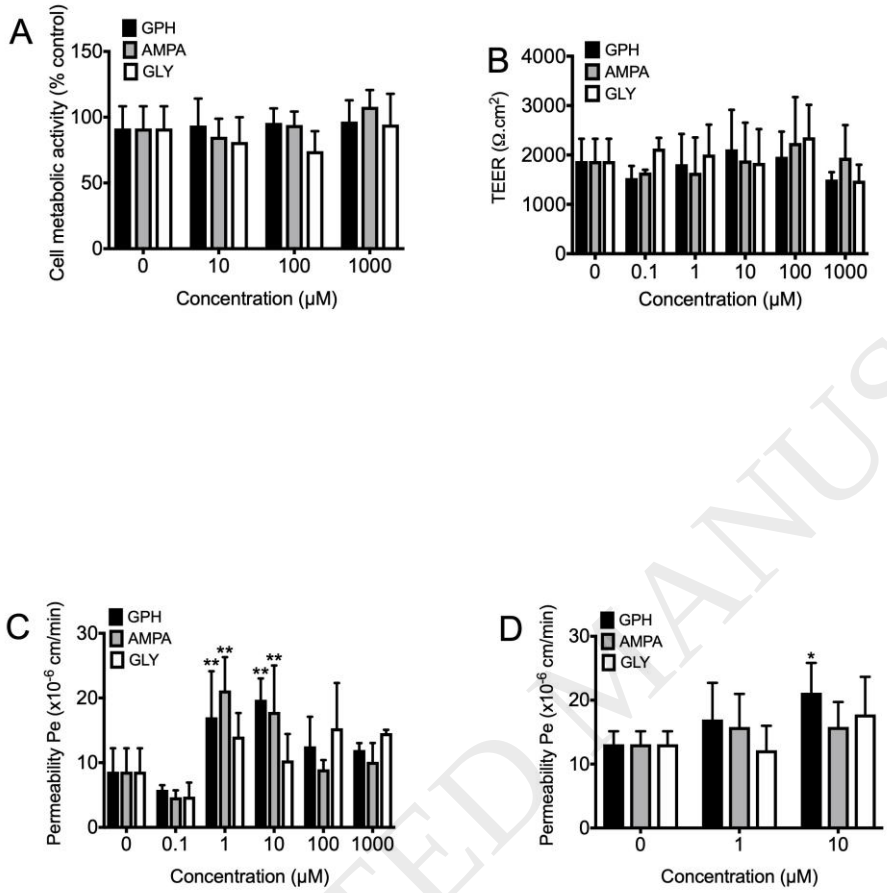

Figure 2: Glyphosate and AMPA reduce tight junction protein levels

(A) Representative micrograph pictures of claudin-5 immunocytochemistry in BMECs monolayers treated for 24 hours. Note the relative absence of protein delocalization from the cell borders. (B) Semi-quantitative analysis of claudin-5 fluorescence intensity. Note the dose-dependent effect of GPH, AMPA and GLY on claudin-5 fluorescence

intensity compared to control. (C) Representative micrograph immunofluorescence and (D) semi-quantitative analysis of occludin localization and expression level. Scale bar = 50μm. N=3 per group, * and ** denotes *P*<0.05 and *P*<0.01 versus control respectively.

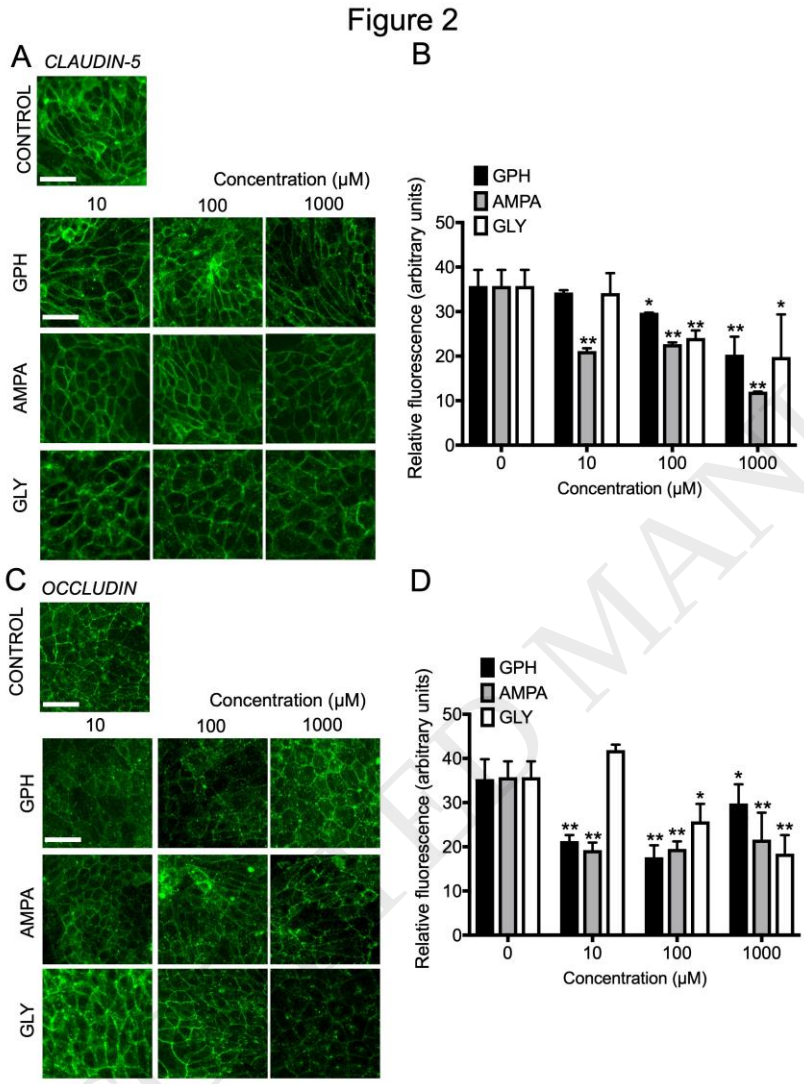

Figure 3: Glyphosate permeability across BMECs monolayers and impact on glucose uptake

(A) Percentage of injected dose (%ID) recovered in the donor (basolateral) chamber after incubation with 100μM GPH in the apical chamber. (B) Permeability profiles of

GPH compared to fluorescein and mannitol. Note the relative higher Pe value observed for GPH compared to two paracellular tracers, suggesting a possible transcellular diffusion.

(C) Effect of 100µM GPH, AMPA and GLY on doxorubicin uptake. Cells were incubated in presence of 100µM for 2 hours before incubation in presence of 10µM doxorubicin. (D) GLUT1 expression profile in iPSC-derived BMECs following 24 hours treatment with GPH, AMPA or GLY. Scale bar=50µm. (E) Semi-quantitative analysis of GLUT1 fluorescence intensity from micrograph pictures. (F) Representative flow cytometry histogram of GLUT1 expression by flow cytometry. Cells treated with mouse IgG isotype served as negative control. (G) Quantitative analysis of GLUT1 mean fluorescence index (MFI, geometric mean) in BMECs following treatment with 100µM GPH, AMPA or GLY. Intrinsic fluorescence index from IgG control were removed from samples. Cells were treated with 100µM for 24 hours, followed by cell detachment and immunolabeling. Note the significant increase in GLUT1 expression (MFI) following treatment with GPH compared to control, whereas GLY has significantly decreased GLUT1 expression. (H) Glucose uptake following 24 hours treatment with GPH, AMPA or GLY. Cells were incubated in presence of 0.4µCi [^{14}C]-D-glucose for 1 hour. Cells were homogenated, intracellular glucose amount was normalized to total protein content by BCA. Note the increased uptake at high levels of AMPA and GLY.N=3, * and ** denote *P<0.05* and *P<0.01* versus controls.

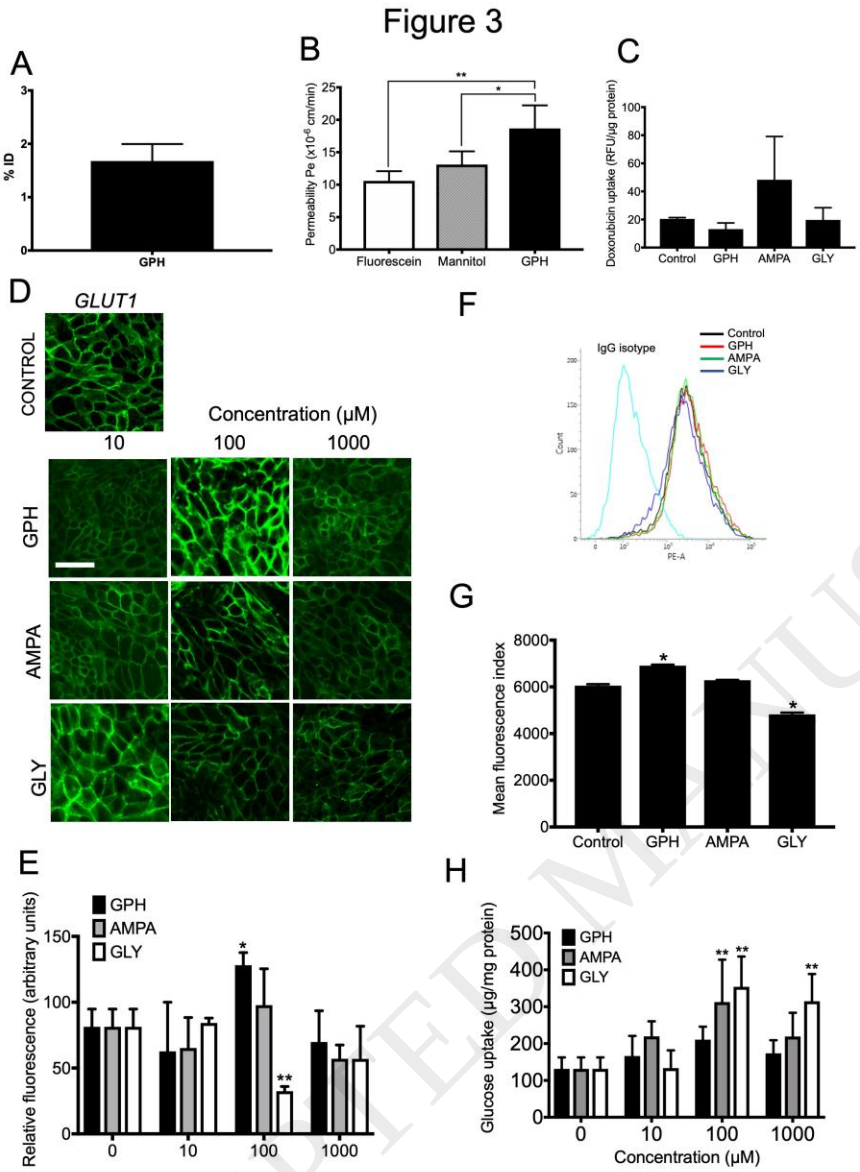

Figure 4: Glyphosate and AMPA induce neurovascular uncoupling in BMECs/neurons co-cultures.

(A) Representative TEER values of iPSC-derived BMECs monocultures or co-cultured with iPSC-derived neurons for 48 hours. Note the 3-fold increase in TEER compared to control. (B) TEER values of co-cultures following 24 hours incubation in presence of GPH, AMPA or GLY in the apical chamber. Both apical and basolateral medium were

replaced prior experiment. (C) Fluorescein permeability of co-cultures after 24 hours incubation. Note the slight increase in GPH compared to control. (D) iPSC-derived neurons cell metabolic activity following co-cultures with BMECs and compared to monocultures. Untreated neurons monocultures served as control for calculation of the cell metabolic activity. Note the increase cell metabolic activity in co-cultures following treatment with 100µM GPH and AMPA treatment, but not observed in the GLY group. N=3 per group, * and ** denote $P<0.05$ and $P<0.01$ versus control. (E) Representative iPSC-derived neurons colonies monocultures and co-cultured with BMECs. Neurites were stained against βIII-tubulin (TUJ1, green), cell nuclei were stained with DAPI (blue). Note the dense neurites processes in both monocultures and co-cultures. GPH or AMPA have no effect on gross morphology. Scale bar = 200µm.

Figure 4

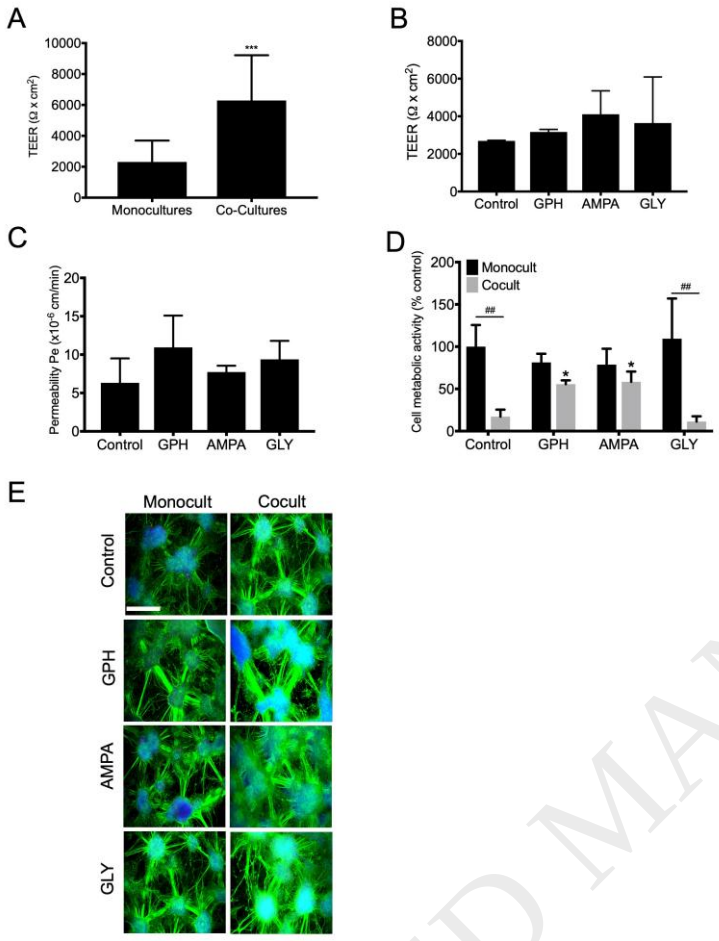

Figure 5: Effect pf glyphosate and AMPA on neuron progenitor cells, differentiating neurons and differentiated neurons.

(A) MTS assay in undifferentiated iPSC-derived neuron progenitor cells (NPCs). Cells were exposed for 24 hours to 0.1 or 1μM concentrations of GPH, AMPA or GLY. Note the significant decrease in cell metabolic activity at 1μM concentration. (B) Representative micrograph pictures of NPCs exposed to 1μM GPH, AMPA or GLY for 24 hours, following staining with nestin. Cell nuclei were counterstained with DAPI (blue). Scale bar = 100μm. (C) Cell metabolic following chronic exposure (16 days).

NPCs were differentiated for 16 days in presence of 0.1μM GPH, AMPA or GLY. Cell medium were replaced every 48 hours. MTS activity was assessed at day 16. (D) Representative micrograph pictures of iPSC-derived neurons at day 16. Note the βIII-tubulin (TUJ1, green) dense neurites network in all groups. Cell nuclei (DAPI, blue) served as counterstain. Scale bar = 200μm.

(E) Effect of acute treatment on differentiated neurons. iPSC-derived NPCs were seeded at low density (50'000 cells/cm^2) to ensure single cells distribution and were matured for 16 days prior experiments. Cells were treated for 24 hours with GPH, AMPA or GLY at various concentrations. Cell metabolic activity on iPSC-derived neurons following 16 days of differentiation. (F) Representative micrograph picture of iPSC-derived neurons exposed for 24 hours. Note the depletion of neurite processes (βIII-tubulin, green) at high GLY concentrations (100 and 1000μM). Cell nuclei were counterstained with DAPI. Scale bar = 50μm. (G) Neuron cell density (as number of cell nuclei per cm^2), note the decrease at 1000μM GPH treatment. (H) Neurites density (neurites per cm^2, normalized to number of nuclei per field). Note the neurite pruning occurring at high concentrations of GLY. N=3, * and ** denotes *P<0.05* and *P<0.01* versus control.

Figure 5